Available online at www.sciencedirect.com
ScienceDirect
Ceramics International 35 (2009) 2853–2869
CERAMICS INTERNATIONAL
www.elsevier.com/locate/ceramint

Chemical durability and microstructural analysis of glasses soaked in water and in biological fluids

V. Cannillo [a], F. Pierli [a], I. Ronchetti [b], C. Siligardi [a,*], D. Zaffe [c]

[a] Dipartimento di Ingegneria dei Materiali e dell'Ambiente, Università di Modena e Reggio Emilia, Via Vignolese 905, 41100 Modena, Italy
[b] Dipartimento di Scienze Biomediche, Università di Modena e Reggio Emilia, Via Campi 287, 41100 Modena, Italy
[c] Dipartimento di Anatomia ed Istologia, Università di Modena e Reggio Emilia, Via del Pozzo 51, 41100 Modena, Italy

Received 2 February 2009; received in revised form 1 March 2009; accepted 20 March 2009
Available online 15 April 2009

Abstract

A new glass, obtained from Bioglass® BG45S5 original composition by substituting CaO with MgO, was produced and its chemical durability and microstructural characteristics were compared with that of Bioglass®.

The two glasses (labelled as BG45 and MG45) were soaked up to 4 weeks at physiological temperature in different solutions, i.e. bi-distilled water, Hank's Buffered Salt Solution 61200 (labelled as HBSS+), Hank's Buffered Salt Solution 14170 (labelled as HBSS−), and Kokubo's SBF. Moreover, the influence of either flat or flake surfaces was analysed for both glasses. Results showed that the chemical durability of a glass in saline at 37 °C, evaluated through pH and ICP-AES chemical analysis of the leached components, depended mainly on the chemical composition of the soaking solution. Moreover, the MG45 glass never exhibited hydroxyapatite crystal formation on its surface also after soaking in calcium-containing solutions. The apatite crystallisation and deposition mechanism, typical of a bioactive glass, was induced only if the glass itself contained calcium. The contemporaneous presence of calcium in the glass and in the soaking solution improved the reactivity of the glass, as apatite crystals nucleated in a shorter time and grew more quickly. As regards the morphology of the glass surface, rougher surfaces favoured the formation of hydroxyapatite crystals on glasses containing calcium.

Keywords: D. Glass; Chemical durability; Calcium; Magnesium; Microstructure

1. Introduction

Bioglass® is the most accepted bioactive glass used in biomedical applications, especially in bone replacement. Hench [1,2] first demonstrated in the 70s that bioactive glasses are able to bind to bone and to promote bone formation. When bioactive glasses are soaked in physiological media or implanted *in vivo*, they can bind to living bone trough an apatite layer formed on their surface. The reaction steps first detailed by Clerk and Hench [3] involve the formation of a silica-rich layer and of a Ca–P-rich layer that crystallises in hydroxyl-carbonate apatite (HCA), a mineral phase similar to that of bone. After the development of Bioglass® by Hench [1,2], with a composition of 45 wt% SiO_2, 24.5 wt% CaO, 24.5 wt% Na_2O and 6 wt% P_2O_5, different bioactive glasses have been produced and studied. Most of them contain both CaO and P_2O_5 as main components [4,5]. Addition of elements, like magnesium or aluminium, may be used to control some physical and chemical properties [6]. It has been found that specific concentrations of magnesium can influence the glass dissolution or the physical–chemical reaction at the glass periphery [7]. Many works analysed bioactive glasses with compositions based on CaO–MgO–P_2O_5–SiO_2 systems [8–13]. Bioactive glasses doped with magnesium lead to the formation of a Ca–P–Mg-rich layer on a pure silica layer. For example, Jallot [6] demonstrated that magnesium influences the spontaneous formation and the evolution of the *in vivo* HCA layer and bone bonding. Moreover, magnesium has a beneficial effect on the crystallinity and on the solubility of apatites. Mg-substituted apatites are more soluble than calcium apatites, and suppress apatite crystallisation in *in vivo* tests [13,14]. Many works have studied the bioactivity, i.e. the HCA deposition,

* Corresponding author. Fax: +39 059 2056243.
E-mail address: cristina.siligardi@unimore.it (C. Siligardi).

0272-8842/$36.00
doi:10.1016/j.ceramint.2009.03.029

mostly by analysing what happens at the surface of a bioactive glass after immersion in a simulated biological fluid (SBF) [15–19]. However, to the best of the authors' knowledge, the present research analyses for the first time the surface reactions in physiological media of phosphate glasses in which the calcium oxide is completely substituted by the magnesium oxide.

In fact, in the present work a glass, based on the composition of Bioglass® 45S5 [1], but modified by the complete substitution of CaO with MgO, has been produced and characterised in comparison to the traditional Bioglass® 45S5. Glasses were soaked in bi-distilled water and in different simulated biological fluids for 1, 2 and 4 weeks, in order to determine the specific effects of Ca^{2+} and Mg^{2+} ions on the chemical durability and behaviour of both glasses and the eventual crystals formation on the surface after incubation in the different media. The physical and the chemical properties of the two glasses were evaluated by using various analytical techniques.

2. Experimental

2.1. Glass systems

The glasses studied in this work were labelled as BG45 and MG45. The BG45 glass had the composition of the 45S5 Bioglass® reported by Hench [1,2] and was chosen as the reference glass. MG45 glass was obtained by substituting CaO by MgO in the composition of BG45. The compositions of the two glasses in wt% and mol% are reported in Table 1. The batch mixtures were prepared from pure grade commercial reagents SiO_2, Na_2CO_3, $CaCO_3$, Na_3PO_4 and $MgCO_3$ (Carlo Erba, Italy). The batches were properly dry mixed by using Al_2O_3 balls for 30 min into porcelain jars. Batches were placed in a platinum crucible and melted in an electric furnace at 1450 °C for 1 h. The melted glasses were then poured into a carbon-made small container to form bulk glasses. The as-cast glasses were then annealed at 560 °C and at 500 °C for 1 h for BG45 and MG45, respectively.

Table 1
Chemical composition of glasses in oxide.

	BG45 (45S5 Bioglass®) [1,2]		MG45	
	wt%	mol%	wt%	mol%
SiO_2	45	46.13	48.33	46.13
Na_2O	24.5	24.35	26.32	24.35
CaO	24.5	26.91	–	–
MgO	–	–	18.91	26.91
P_2O_5	6	2.60	6.44	2.60

Glasses were cut to dimensions of 5 mm × 5 mm × 3 mm, polished to a 0.5 μm finishing using diamond paste and then washed with acetone in an ultrasonic bath. To evaluate the effect of the surface morphology of glasses on their chemical durability, flake samples were also prepared, without polishing: in this way the surface was rough. Comparison of the roughness between flat and flake surfaces was made by means of an optical profilometer (Conscan Profilometer, CSM Instruments). All samples were stored in a desiccator until used.

The glasses were characterised by means of DTA analysis (Netzsch DSC 404 Differential Thermal Analyzer), using 30 mg of powders heated from 20 °C to 1400 °C at 10 °C/min, in order to obtain the critical temperatures of glasses, such as glass transition and crystallisation temperatures (accuracy of DTA = ±2 °C). Density measurements were performed through He picnometry (AccuPyc 1330, Micromeritics) and the molar volume was calculated in order to evaluate the effect of replacing CaO with MgO on the structure of glasses. The molar volume (V_m) was calculated from the density data obtained by using the following relation [20]:

$$V_m = \sum_i \frac{Mi\,Ni}{\rho}$$

where Mi and Ni are the molar weight and the molar ratio of the oxide, respectively.

2.2. Dissolution study and microstructural characterisation

The flat glasses were immersed into four different fluids: bi-distilled water, Hank's Buffered Salt Solution 61200 (labelled as HBSS+), Hank's Buffered Salt Solution 14170 (labelled as HBSS−) and SBF (Simulated Body Fluid). The SBF was prepared and used according to the procedure described by Kokubo and Takadama [21]. HBSS+, HBSS− and SBF have composition similar to human body fluids, as reported in Table 2 [21,22]. The HBSS+ solution was characterised by a little amount of Ca^{2+} and Mg^{2+}, while the HBSS− solution was free of Ca^{2+} and Mg^{2+}. Since a previous work [23] showed that the surface morphology of bioactive glasses significantly influences their physiological performance, in the present study, the *in vitro* bioactivity of the two glasses with either flat or rough surfaces was compared after soaking in SBF, as this is the most accepted solution for *in vitro* tests [21].

Glasses were soaked in 2 ml of solution (four different tests for each glass: water, HBSS+, HBSS−, and SBF) for 1, 2 and 4 weeks at a constant temperature of 37 °C in a cell culture incubator. Tests were carried out in duplicate. Measurements of

Table 2
Ion concentration (mM) and pH of SBF, HBSS+, HBSS− in comparison with human blood plasma.

	Na^+	K^+	Mg^{2+}	Ca^{2+}	Cl^-	HCO_3^-	HPO_4^-	SO_4^-	pH
Human body plasma	142	5	1.5	2.5	103	27	1.0	0.5	7.40
SBF	142	5	1.5	2.5	147.8	4.2	1.0	0.5	7.40
HBSS+	81	4.6	0.97	1.4	85.4	–	1.08	–	6.80
HBSS−	84.5	4.6	–	–	84	3.5	1.08	–	7.81

pH (accuracy of ±0.01) were taken at 37 °C, after each soaking interval, by means of a pH meter (Crison, MicropH). The pH measurements of different solutions were correlated to the dissolution of ions in the incubation media. Changes in the concentration of Si^{4+}, Na^{+}, Ca^{2+} and Mg^{2+} within the soaking solutions were measured by inductively coupled plasma atomic emission spectrometry (ICP-AES). Standard sample concentrations were measured periodically to ensure the accuracy of the calibration curve.

Microstructural characterisation was carried out by a scanning electron microscope (ESEM Quanta-200, coupled with EDS Oxford INCA 350), in low vacuum mode (at pressure of 1 Torr). The specimens were observed by ESEM/EDS before and after soaking in different solutions. The surfaces were observed after careful rinsing in distilled water and without metallization for not altering the surfaces. XRD analyses (X'PERT PRO) were carried out by XRD in the 15–80° range, at a speed of 2°/min with 0.02° increment, using Cu-Kα at 40 kV and 40 mA, in order to analyse the crystalline phases formed after soaking in different fluids.

3. Results and discussion

3.1. Glass characterisation

The BG45 and MG45 glasses had a density of 2.718 ± 0.001 g/cm^3 and of 2.562 ± 0.002 g/cm^3, respectively. Magnesium belongs to the lightest elements (Li, Mg, Be, and B), therefore the density of glasses decreased by the introduction of MgO instead of CaO [24,25].

The calculated molar volume of BG45, containing CaO, was 22.63 cm^3/mol, while the molar volume of MG45 glass, containing MgO, was 22.38 cm^3/mol. It is interesting to note that at higher density corresponded higher molar volume, even if the molar volumes of the two glasses were rather close. The small differences could be explained in terms of the cation field strength of oxides present in the glass. The cation field strength is given by:

$$F = \frac{Z}{d^2}$$

where Z is the modifier charge and d is the cation–oxygen (M–O) distance [20]. According to Dietzel criterion [26], the network-forming cations have field strength about 1.5–2, the network-modifying cations have field strength of about 0.1–0.4, and those having field strength values between 0.5 and 1.1 are intermediate cations. In the case of the cations in BG45 and MG45 glasses, the field strength increases in the order Na (0.18), Ca (0.36) and Mg (0.46–0.53) [25,27]. This indicates an increase in bond strength in the order of Na–O, Ca–O, Mg–O. Since the cations with a low field strength can come close to each other [20], the higher is the cation field strength, the lower is the molar volume of the glass. Therefore, the calculated values of molar volume are coherent with the cation field strength of oxides in the two glasses: in fact at the higher molar volume of BG45 glass corresponds the lower cation field strength of CaO.

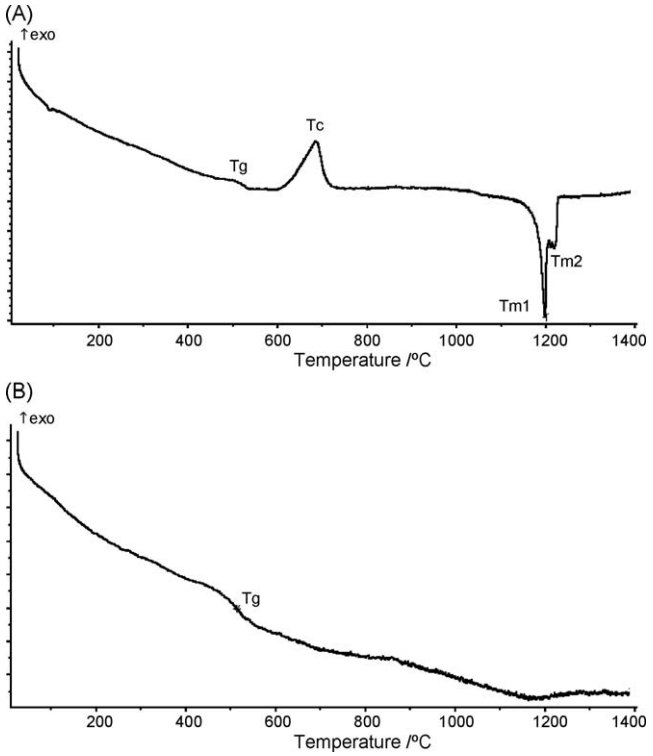

Fig. 1. Differential thermal analysis of (A) BG45 glass and (B) MG45 glass (heating rate 10 °C/min).

Differential thermal analysis, reported in Fig. 1, indicates that the BG45 glass had a T_g at around 522 °C. The DTA curve (Fig. 1A) showed one exothermal crystallisation peak (T_c), at around 687 °C. These features had already been observed in previous studies [28–30]. Two endothermic peaks (T_{m_1} and T_{m_2}), at 1200 °C and 1230 °C, corresponded to the melting of two crystalline phases, as previously reported in the literature [29]. The DTA of the MG45 glass (Fig. 1B) was completely different from that of BG45 glass. The MG45 glass had T_g at 530 °C and the DTA curve did not show any exothermal crystallisation peak. The MG45 glass was more thermally stable in comparison with the BG45 glass. Previous works [24] demonstrated that, in the Na_2O–CaO–SiO_2 system, the presence magnesium oxide decreased considerably the rate of crystallisation; in particular the addition of 2.5 wt% of MgO resulted in a sharp minimum of crystallisation. The crystallisation properties decrease again when the MgO content exceeds 5 wt%, such as in MG45 (containing 18.91 wt% of MgO). The transition temperatures (T_g) of the two glasses were similar, since T_g were 522 ± 2 °C and 530 ± 2 °C for BG45 and MG45, respectively. Therefore, the complete substitution of calcium oxide with magnesium oxide did not substantially modify the glass network structure.

The surfaces of the glasses before soaking are reported in Fig. 2, which shows the ESEM images of BG45 and MG45 glasses (Fig. 2A and C) and the corresponding EDS spectra (Fig. 2B and D) confirming the chemical compositions of the two glasses. The flat glasses did not show any defect and other

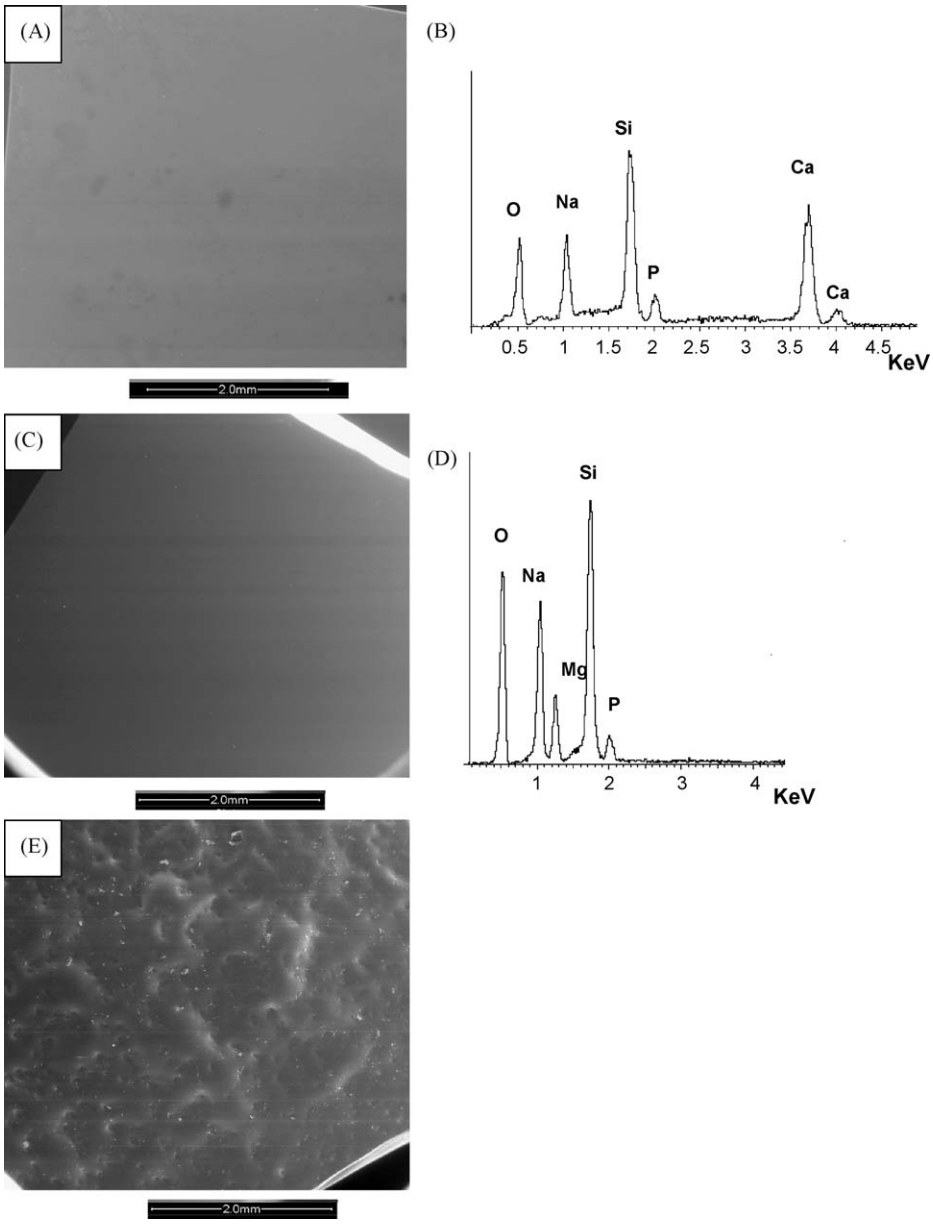

Fig. 2. SEM images and EDS spectrum of glass surfaces before soaking. (A and B) BG45 in flat form, (C and D) MG45 in flat form, and (E) BG45 in flake form.

relevant features (Fig. 2A and C); by contrast, the flake samples had a rough surface (Fig. 2E). The average arithmetic roughness (Ra) of the surface of flat samples was about 0.50 ± 0.10 μm and 1.30 ± 0.21 μm, for BG45 and MG45 glasses, respectively. The Ra of the surfaces of the flake samples was about 7.18 ± 0.67 μm and 6.47 ± 0.53 μm, for BG45 and MG45 glasses, respectively.

3.2. Dissolution analysis

3.2.1. Incubation in bi-distilled water

The change in pH of the solution after soaking BG45 and MG45 glasses in bi-distilled water is reported in Fig. 3A. The pH variation with time was quite similar for both glasses. The pH increased during the first period of incubation for both BG45 and MG45, then remained quite constant with time. In particular, the pH increased very rapidly from 6.1 to around 8.7 and 10.2 in a week for MG45 and BG45 respectively, reaching an equilibrium in the next weeks. Solutions were always basic for both samples, due to a basic ion transfer from glasses to water. Because alkali ions are the most mobile ions in the glass, leaching of alkali ions, such as Na^+, Mg^{2+} and Ca^{2+}, influences the chemical durability [24]. Previous works had already shown that a rapid ion exchange of H^+ and H_3O^+ from the solution to the glass and of Na^+ from glass to the solution occurred during soaking in bi-distilled water [1,31]. In the present study, exchange of Na^+/H^+ ions, confirmed also by ICP data, was very rapid during the first week and, then, reached an equilibrium, corresponding to a gradual dissolution of the glass network. However, the pH of the BG45 glass solution was always more

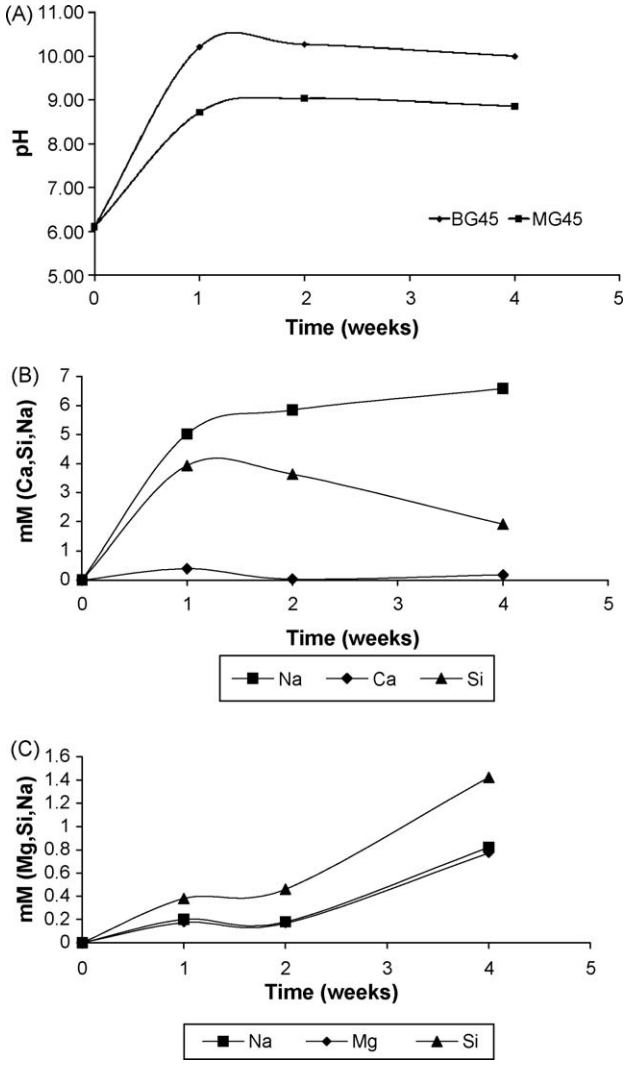

Fig. 3. (A) Change in pH of BG45 and MG45 after soaking in bi-distilled water for specific time intervals. (B and C) Ion release from BG45 (B) and MG45 (C) after soaking in bi-distilled water.

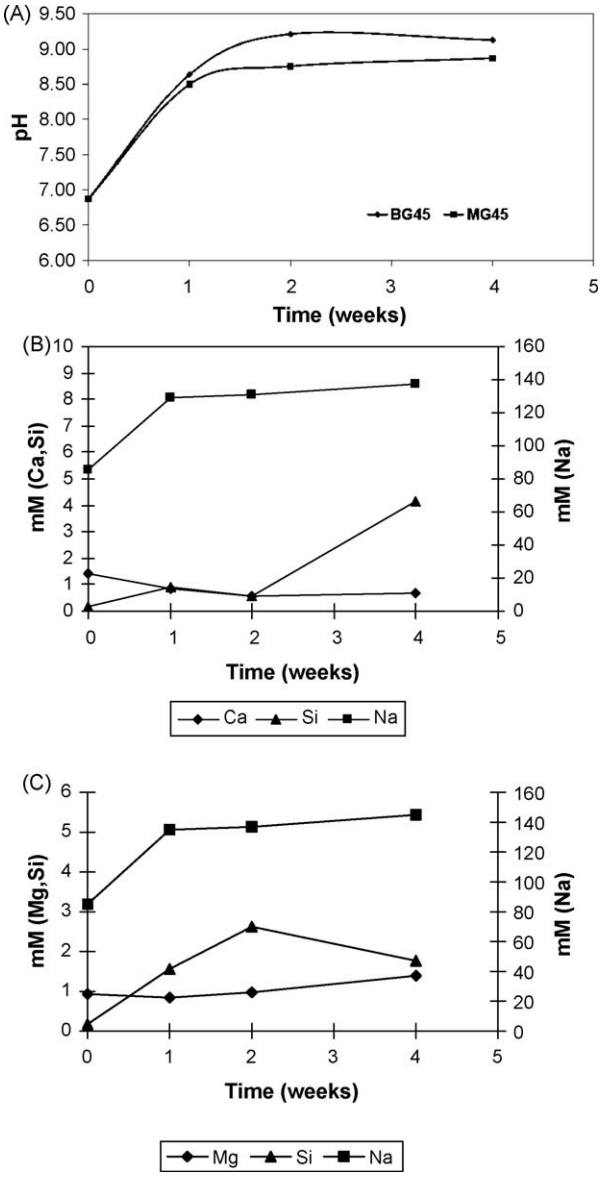

Fig. 4. (A) Change in pH of BG45 and MG45 glasses after soaking in HBSS+ for specific time intervals. (B and C) Ion release (mM) of BG45 (B) and MG45 (C) glasses after soaking in HBSS+ for specific time intervals.

basic than that of the MG45 glass solution. This could be due to the lower ion exchange in MG45 glass. Fig. 3B and C shows the ICP results of the dissolution of BG45 and MG45 glasses in bi-distilled water for a 4-weeks soaking. The results were presented as the millimolar concentration measured in the solution. The higher values of silicon release from BG45 compared to MG45 (i.e. maximum silicon release value of 4 mM and 1.5 mM, respectively) could be explained by the higher pH reached in the solution of BG45 which increased the silica solubility and promoted the nucleophilic attack of SiO_4 units by OH^- [32]. The final value of Si^{4+} release from BG45 after 4 weeks of soaking was lower due to the SiO_2 crystallisation. The Na^+ release was faster for BG45, reaching a final concentration of about 6.5 mM after 4 weeks, while for MG45 the Na^+ release was slower, with a maximum concentration of about 0.8 mM. The Ca^{2+} release of BG45 was slow in water, probably due to the formation of Ca-containing salts, i.e. calcium carbonate, which are less soluble at higher pH, as reported by Cerruti et al. [18]. The ions leaching out from BG45 (reported in Fig. 3B) was similar to that reported in the literature [18]. The ions release from MG45 (Fig. 3C) was always lower in comparison to the ions release from BG45, coherently with the pH behaviour of BG45, which is more basic than the pH of MG45. Nevertheless, the release of silicon, sodium and magnesium always increased with time. This increase in leaching of mobile ions out from a glass can be attributed to a uniform superficial dissolution of the glass network and to a difficult precipitation of insoluble compounds.

The ICP analysis of the leachate from the two glasses demonstrated that the chemical durability in water of MG45 was higher in comparison with that of BG45. In order to compare the chemical durability of the two glasses, it is interesting to consider their chemical compositions—from which their properties depend. The glasses of the present study belong to a large family of multi-component glasses

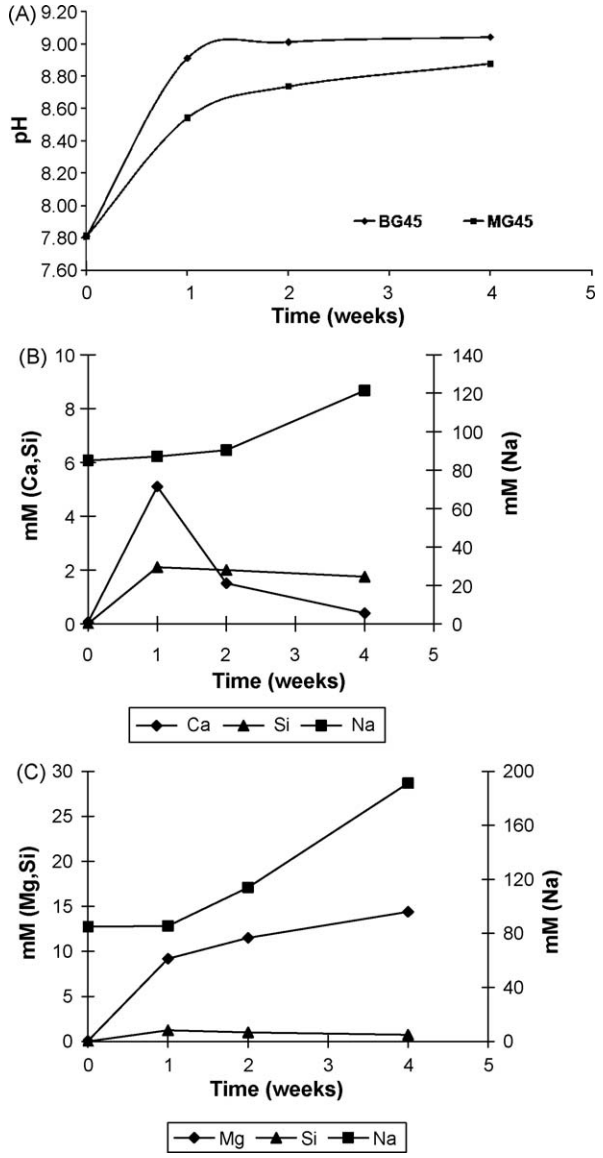

Fig. 5. (A) Change in pH of BG45 and MG45 glasses after soaking in HBSS− for specific time intervals. (B and C) ICP data for BG45 (B) and MG45 (C) after soaking in HBSS− for different times.

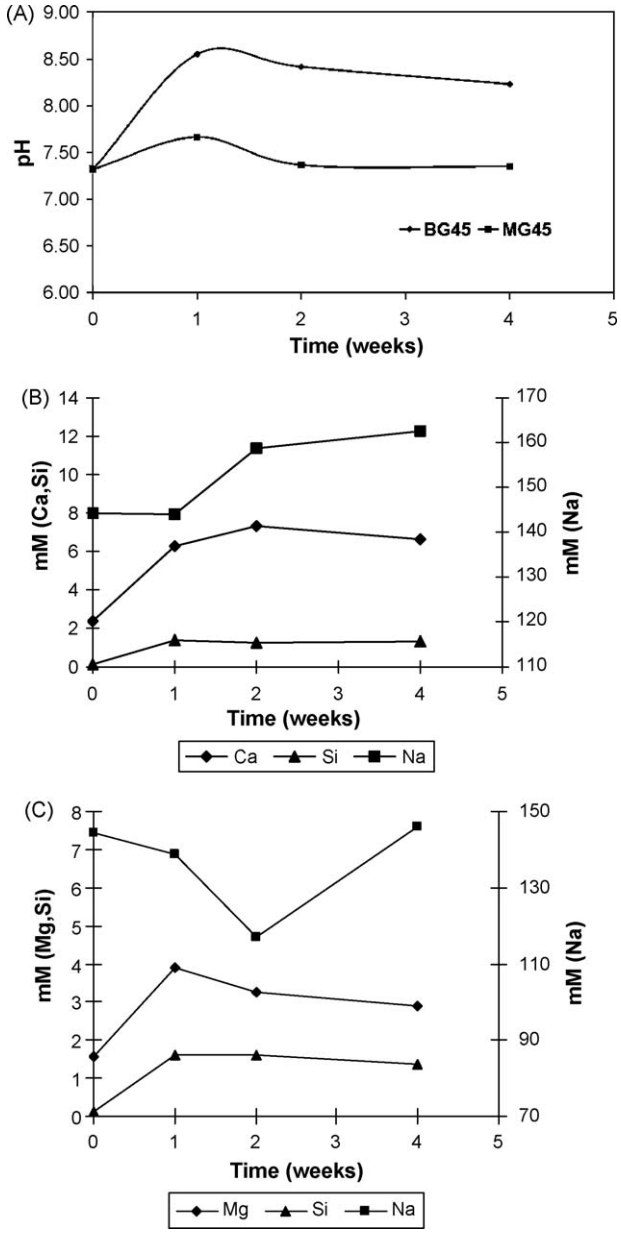

Fig. 6. (A) Change in pH of BG45 and MG45 flat glasses after soaking in SBF for specific time intervals. (B and C) ICP data for BG45 (B) and MG45 (C) glasses after soaking in SBF for different times.

characterised by the co-presence of silicon and phosphorous that act as network-former cations. The solubility of the present glasses was not affected by the concentration of network-formers but mostly by the concentration of network-modifiers: in fact the addition of network-modifiers disrupts bonds, lowering the cross-link density and increasing the number of non-bridging oxygen atoms present in the glass. Divalent cations, such as Ca^{2+} or Mg^{2+}, can serve as ionic cross-links between the non-bridging oxygen atoms of two phosphate chains. Therefore, the chemical durability decreases as the mole fraction of CaO or MgO in the glass is decreased in exchange for monovalent Na^{+} modifier cations, as ionic cross-links are disrupted [33,34]. The better chemical durability of MG45 could be attributed to the higher cation field strength of the Mg–O linking in comparison with the Ca–O linking [25].

3.2.2. Incubation in HBSS+

Fig. 4A illustrates the time-dependent change of pH in the HBSS+ solution after soaking BG45 and MG45 glasses. The pH behaviour of the two glasses was similar, since pH immediately increased for both glasses from 6.8 to about 8.5 during the first week and then remained quite constant. The increase was probably due to an ion exchange of alkali ions from glasses to the solution, as shown by previous studies describing the surface reactions of alkali-containing silicate glasses exposed to a water environment [24,35,36]. These studies demonstrated that there is a two-stage reaction, involving dealkalization of the surface by exchange of a H^{+} ion with an alkali ion, followed, at higher pH (>10), by

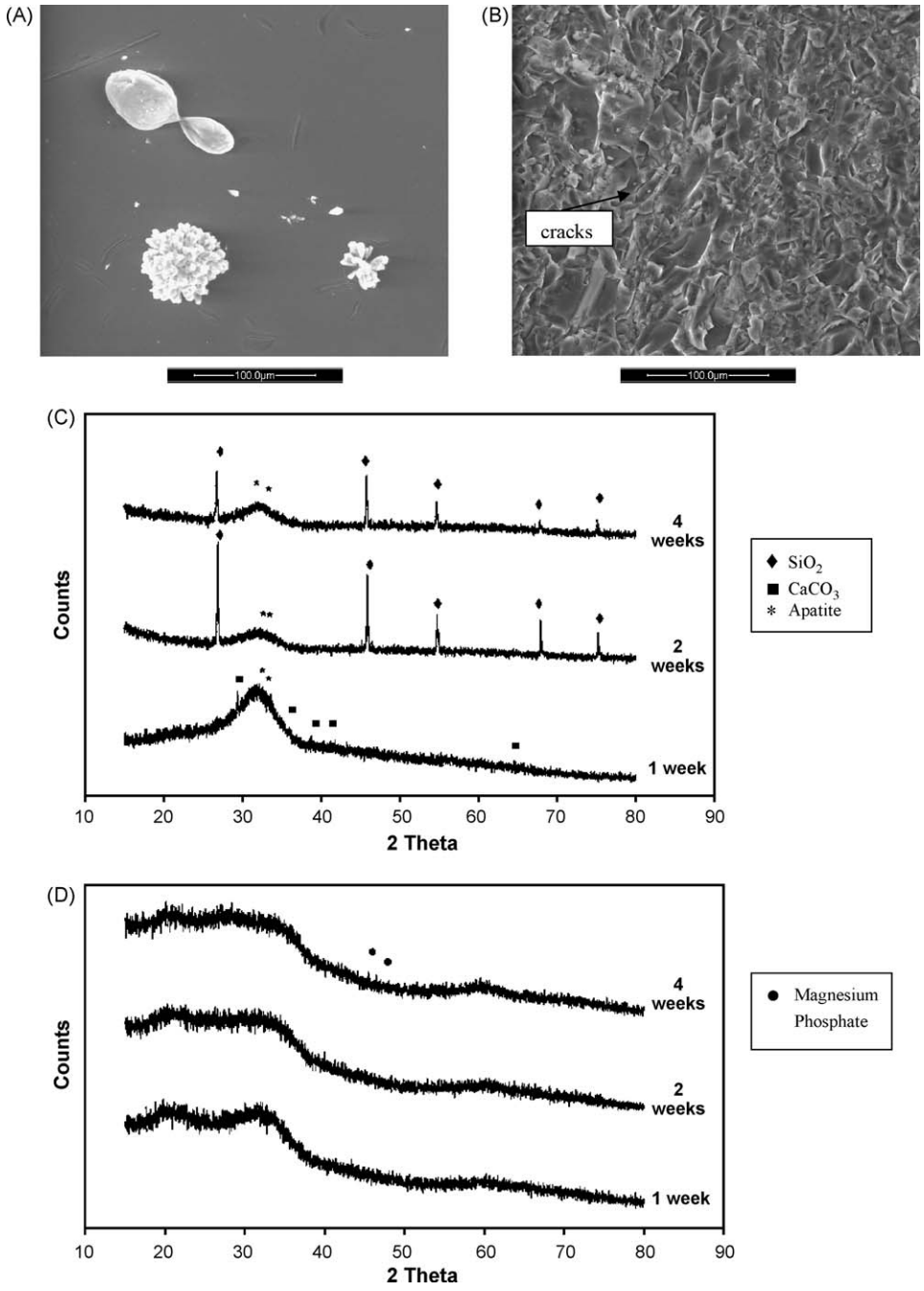

Fig. 7. (A and B) SEM images of BG45 and MG45 glass surfaces after soaking in bi-distilled water: (A) BG45 after 1 week, (B) MG45 after 1 week. (C and D) XRD spectra of BG45 (C) and MG45 (D) after soaking in bi-distilled water.

the network dissolution due to hydroxyl ion breakdown of Si–O–Si bonds. Fig. 4B and C shows the results of the ion release from BG45 and MG45 in HBSS+ at different times of soaking. The silicon release presented a plateau at about 1 mM, corresponding to a pH value <9; later, it increased to a maximum value of 4 mM after 4 weeks for BG45.

The silicon release from the MG45 glass increased until the second week of soaking, reaching the concentration of 2 mM, then decreased, probably corresponding to silica precipitation. The higher maximum value of Si^{4+} observed in BG45 can be explained by the increase of silica solubility at pH higher than 9 [18].

The Na^+ release from BG45 and MG45 glasses was similar, reaching values of 140 mM, much higher than the values of other released ions. The pH increase with time (Fig. 4A) was mainly attributed to the exchange of Na^+ from the glass to the solution. The slow release of Ca^{2+} from BG45 could be attributed to the precipitation of apatite crystals on the surface of samples, as shown by microstructural analysis (see Section 3.3). In conclusion, when incubated at 37 °C in a calcium-containing medium, the chemical durability of the

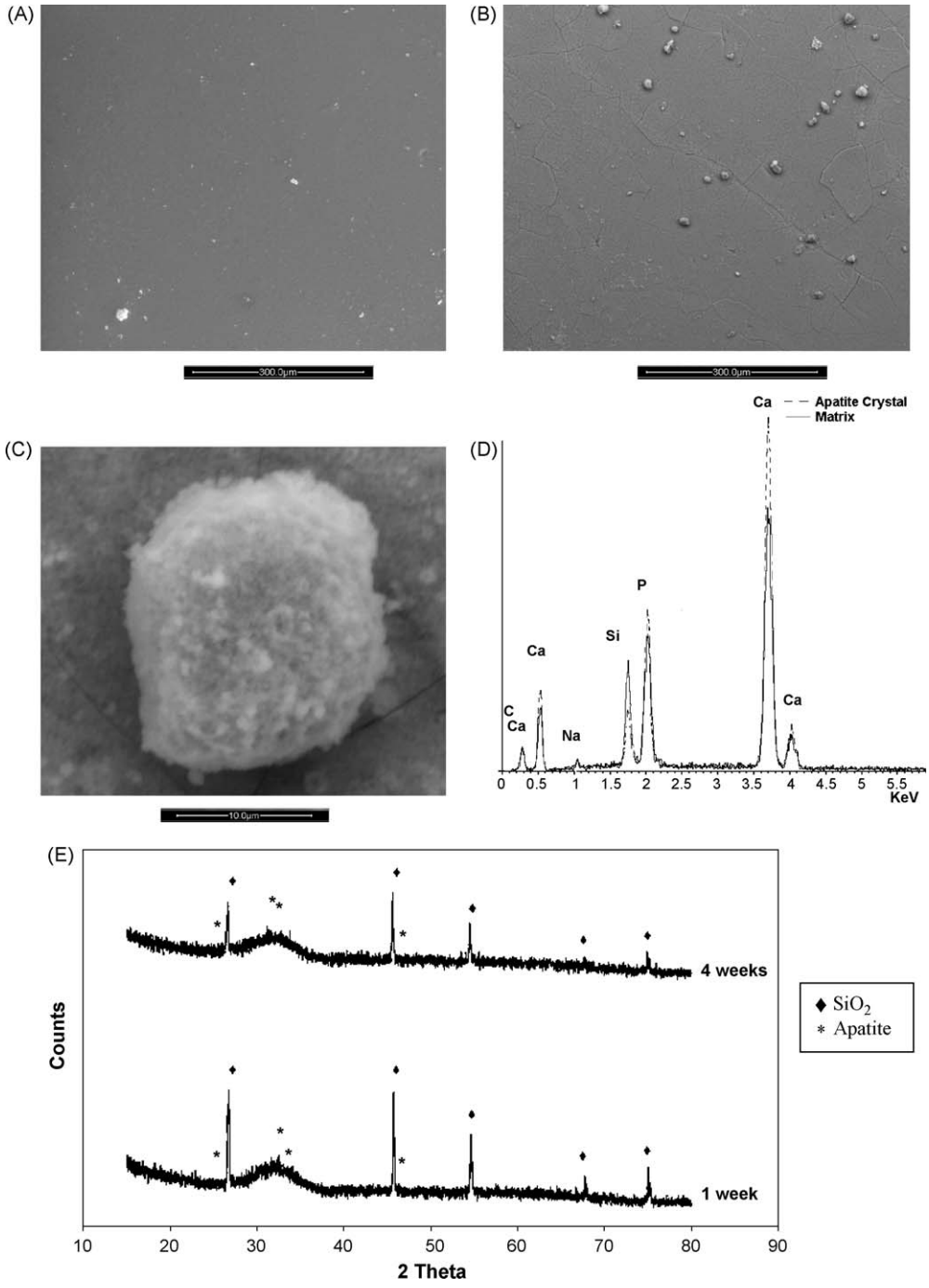

Fig. 8. (A and B) SEM images of BG45 glass surfaces after soaking in HBSS+: (A) 1 week, (B) 2 weeks. (C and D) Particular of a crystal after 4 weeks and corresponding EDS spectrum. (E) XRD spectra of BG45 glass after soaking in HBSS+ for different times.

two glasses, in term of leachate from ICP-AES analysis, was similar.

3.2.3. Incubation in HBSS−

The change in pH of BG45 and MG45 glasses versus time of soaking in HBSS− was reported in Fig. 5A. The pH behaviour of the two glasses was similar, since the pH immediately increased after the first week of soaking for both the glasses. The immediate pH increase from 7.81 to about 8.91 and 8.54, for BG45 and MG45 respectively, was attributed to an alkali ion exchange, as confirmed by ICP-AES results in Fig. 5B and C. Even if the alkali ion release continued after the second week of soaking (in particular sodium release), a plateau of the pH was reached. The phenomena could be attributed to a gradual dissolution of the glass network. The sodium release from BG45 and MG45 was similar, but the maximum value reached for MG45 was higher than the value for BG45 (180 mM instead of 120 mM). The silicon behaviour was the same for both glasses. Silicon increased in the solution after the first week

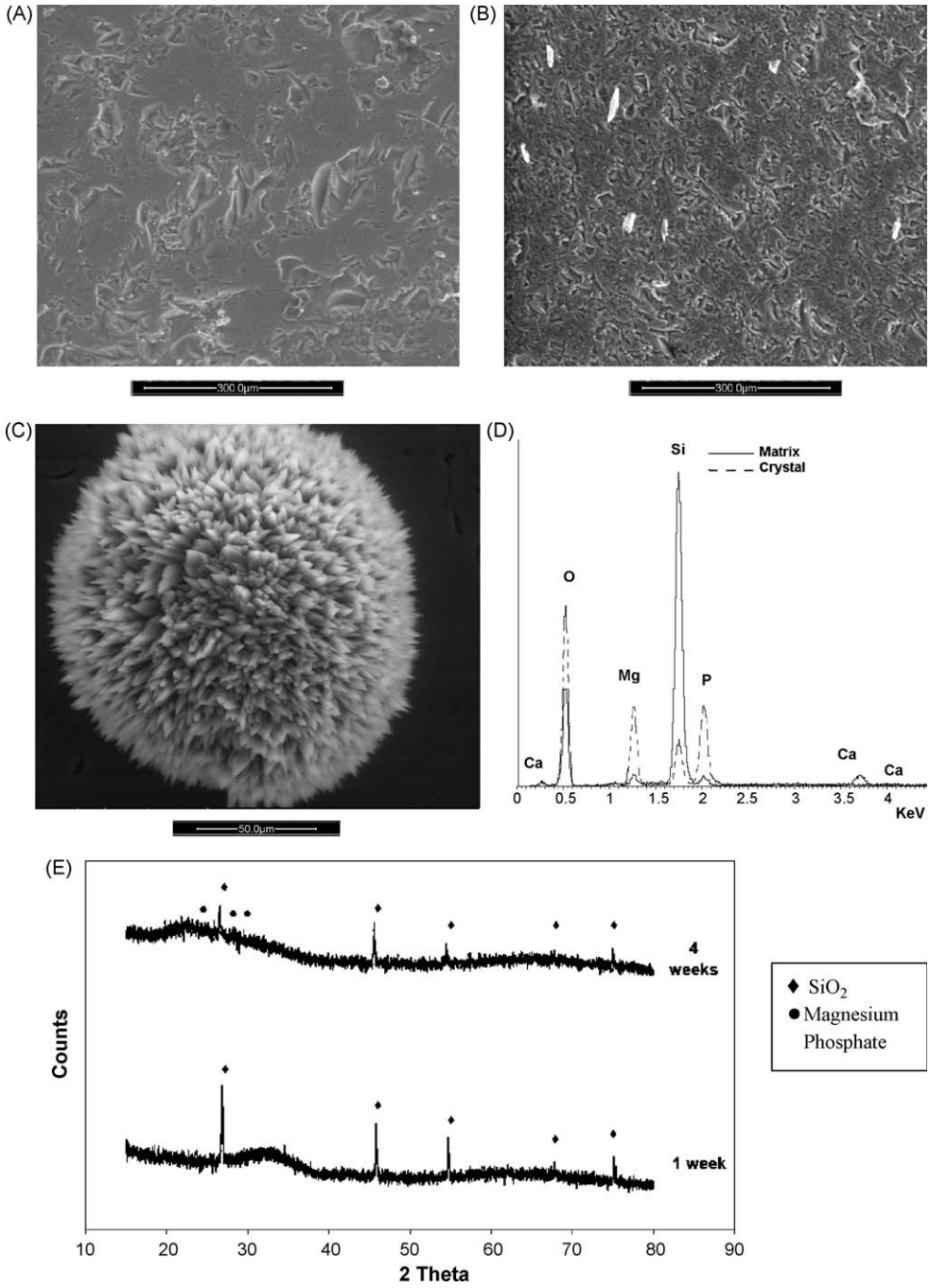

Fig. 9. (A and B) SEM images of MG45 glass surfaces after soaking in HBSS+: (A) 1 week and (B) 2 weeks. (C and D) Particular crystal after 4 weeks and corresponding EDS spectrum. (E) XRD spectra of MG45 glass after soaking in HBSS+ for different times.

of soaking, reaching a plateau at 2 mM, corresponding to an equilibrium between the glass and the solution. The Ca^{2+} release from BG45 glass increased dramatically during the first week of soaking, then the calcium ion concentration decreased in the soaking solution probably due to the formation and precipitation of apatite crystals. The Mg^{2+} release from MG45 was higher in comparison with the Ca^{2+} release from BG45. The chemical durability of BG45 was slightly higher than that of MG45, because of the smaller ion release.

3.2.4. Incubation in SBF

The change in pH of the SBF solution after the soaking of glasses is illustrated in Fig. 6A. During the first week, the pH of the solutions increased for both glasses and then slowly decreased. The pH increase for MG45 was always lower than that for BG45, being the maximum pH values 8.6 and 7.4 for BG45 and MG45, respectively. The increase of pH was associated with the first stage of reactions of the surface dealkalization. Later, the network dissolution stage tended to dominate [35].

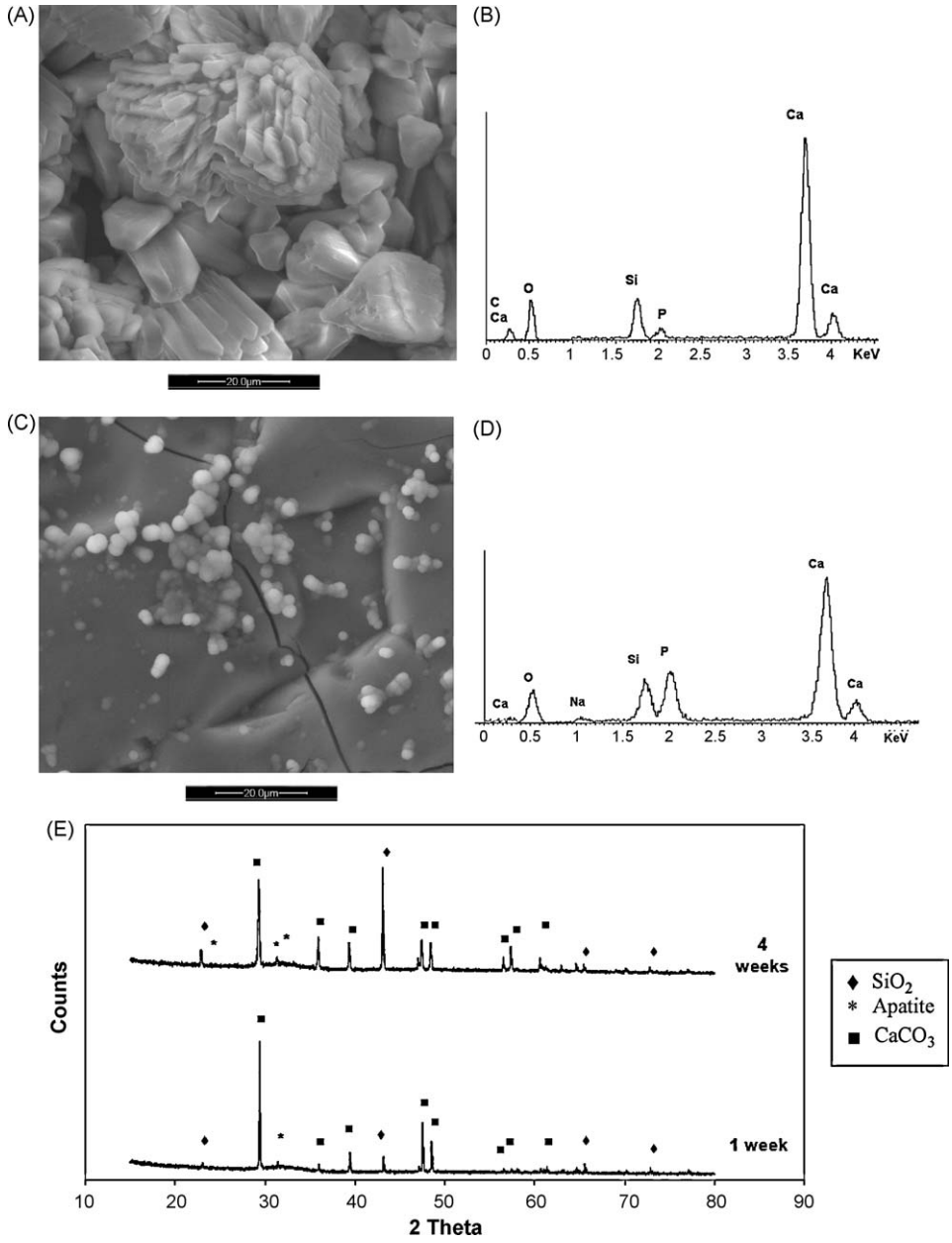

Fig. 10. SEM images of BG45 glass surfaces after 4 weeks of soaking in HBSS−: (A and B) $CaCO_3$ crystals and corresponding EDS spectrum. (C and D) Apatite crystals and corresponding EDS spectrum. (E) XRD spectrum of BG45 after soaking in HBSS−.

The ICP-AES data of the dissolution of BG45 and MG45 in SBF with time is illustrated in Fig. 6B and C, respectively. The Si^{4+} release was low for both BG45 and MG45, having a similar trend with a plateau at 1 mM. Also the Na^+ release had a similar behaviour for both glasses, with a plateau at 140–150 mM. It is interesting to note that the maximum value of Na^+ concentration was much higher compared with the maximum value of the other ions. Therefore, the initial increase in pH can be attributed mainly to the Na^+ ion exchange from the glass to the fluid. The Ca^{2+} release from BG45 was fast in the first and second weeks of soaking, then calcium ions in solution decreased, probably due to apatite crystallisation on the surface of BG45 (see microstructural analysis in Section 3.3). The Mg^{2+} ions were released in the first week of soaking from MG45; the release was slower during the second week in SBF, probably corresponding to a magnesium-based crystal formation, as shown by the microstructural analysis (Section 3.3).

The chemical durability of MG45 was better than that of BG45, since the leachate from BG45 was higher.

The chemical durability of flat and flake samples in SBF was similar both for MG45 and BG45, since the pH trend of flake glasses was similar to that of flat glasses (not reported). The AES-ICP analysis confirmed the same ions release from flake and flat samples (data not reported, for sake of brevity and conciseness).

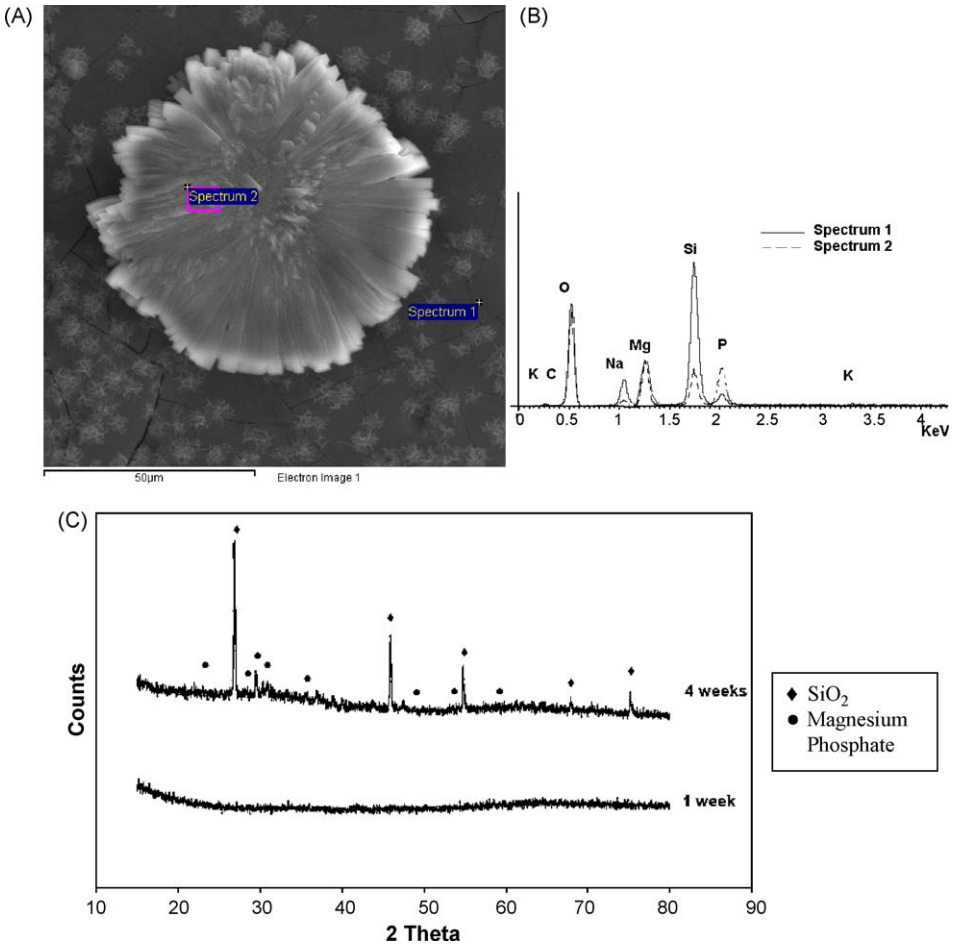

Fig. 11. (A and B) SEM surface image and EDS spectrum of crystals on MG45 surface after 4 weeks of soaking in HBSS−. (C) XRD spectrum of MG45 glasses after soaking in HBSS−.

3.3. Microstructural characterisation

3.3.1. Microstructural analysis in bi-distilled water

After 1 week of soaking in bi-distilled water at physiological temperature, BG45 underwent a superficial corrosion, due to the leaching of alkali ions from glass to the solution. Moreover, some crystals grew on the glass surface (Fig. 7A); such crystals were very rich in calcium, while the matrix was rich in silicon, as revealed by EDS. The crystals were made of calcium carbonate ($CaCO_3$, JCPDS 47-1743), as shown by the XRD spectrum (Fig. 7C). Calcium carbonate had a strong tendency to precipitate in water, as the solubility index of $[Ca^{2+}][CO_3{}^{2-}]$ is about 4.96×10^{-9}, which is lower in comparison with that of $[Ca^{2+}][OH^-]^2$, which is about 4.68×10^{-6}. Moreover, calcium carbonate precipitation was promoted by the presence of $HCO_3{}^-$ in water, due to the interaction of water with atmospheric CO_2. This was confirmed by the pH 6 (slightly acidic) of the solution at the beginning of the test. The $CaCO_3$ crystals were detected by X-rays only after the first week of soaking. Later, they probably became bigger and were removed during the post-rinsing in water, necessary to eliminate some soluble salts, such as NaCl, from the surface of glass. The XRD spectrum showed that SiO_2 (JCPDS 79-1906) was the main phase in the surface of BG45 glass (Fig. 7C). Actually, the upper layer of BG45 was rich of SiO_2 nanocrystals, detected by XRD, but not visible by ESEM.

Numerous cracks were observed on the surface of MG45 immediately after immersing in bi-distilled water (Fig. 7B). The predominant surface reaction was the uniform dissolution of the glass network. The surface appeared corroded and etched, and no crystals were visible. The XRD analysis (Fig. 7D) showed that no compounds were formed on the surface of MG45 after contact with bi-distilled water, except for traces of magnesium phosphate crystals (JCPDS 5-0579) found after 4 weeks soaking. The precipitation in a basic environment of magnesium phosphate salts instead of magnesium carbonate or magnesium hydroxide was expected since the solubility index of $[Mg^{2+}]^3[PO_4{}^{3-}]^2$ is about 9.86×10^{-25}, lower than the solubility index of $[Mg^{2+}][CO_3{}^{2-}]$ of about 6.82×10^{-6} and of $[Mg^{2+}][OH^-]^2$ of about 5.61×10^{-12}.

3.3.2. Microstructural analysis in HBSS+

After 1 week immersion in HBSS+, some small crystals were seen on the surface of BG45 (Fig. 8A). These crystals became larger after 2 and 4 weeks of soaking (see Fig. 8B and C) and were richer in phosphorous and calcium, compared to the glass matrix, as shown by the EDS spectrum (Fig. 8D). The Ca/P ratio in crystals was 2.07 and 1.58 after 2 and 4 weeks

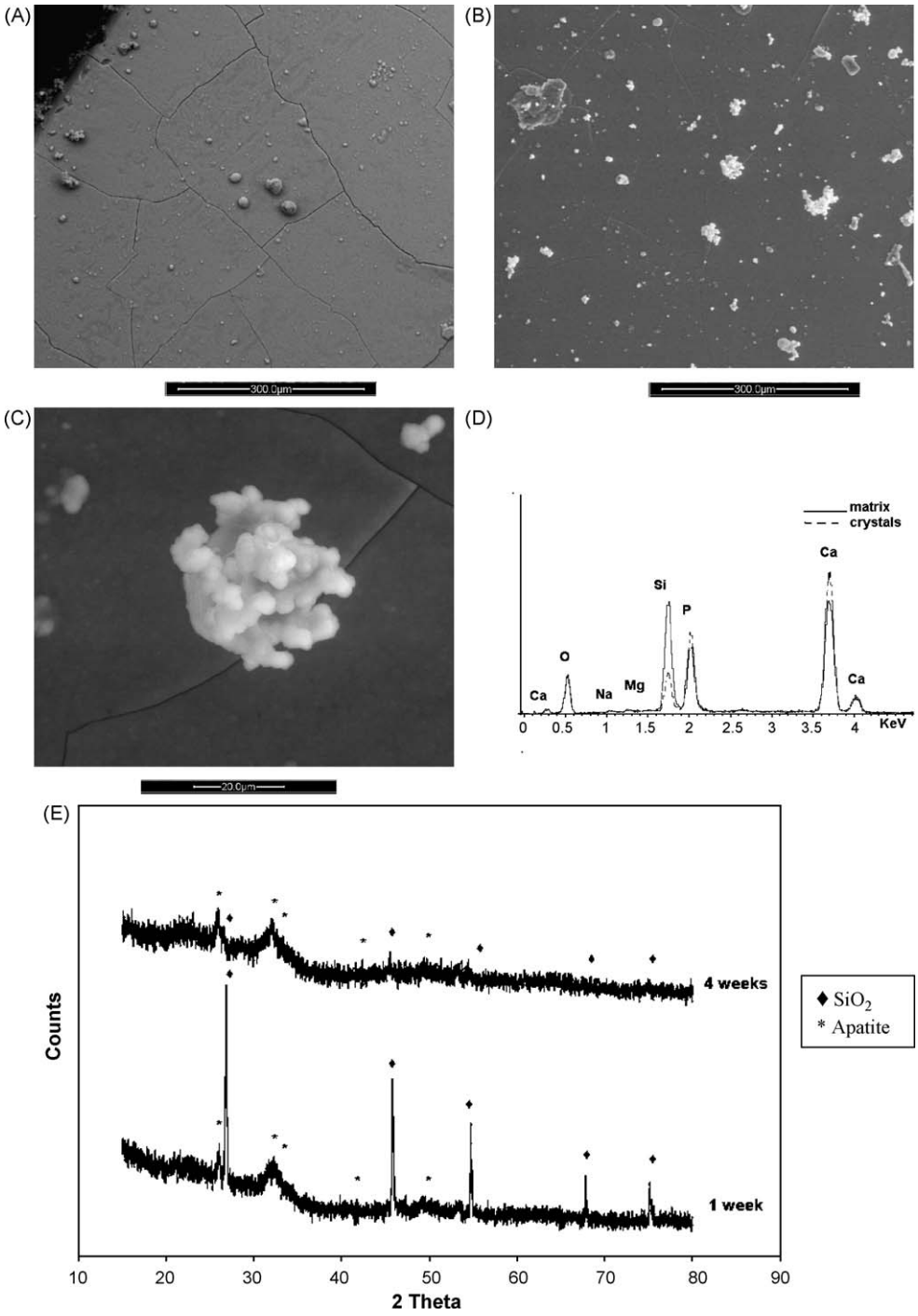

Fig. 12. (A–D) SEM images of BG45 glass flat surfaces after soaking in SBF: (A) 1 week, (B) 2 weeks, (C and D) particular of a crystal after 4 weeks and corresponding EDS spectrum. (E) XRD spectra of BG45 after soaking in SBF.

incubation respectively (semi-quantitative analysis from the EDS spectra). Therefore, the Ca/P ratio of the apatite crystals found in the present work is close to that reported in the literature of 1.67 (ISO 13779-3 standard) for hydroxyapatite. These apatite crystals were also detected by X-rays after 4 weeks of soaking (Fig. 8E). Nevertheless, the major peaks in XRD spectrum were always those of SiO_2 (JCPDS 79-1906). However, the bioactive mechanism seems to be similar to that reported in literature [2]. It would consist of a SiO_2-rich layer covered by an HCA layer [1,17]. These two layers would form a protective film and the BG45 surface would be of type III, as classified by Hench and Clark [35], with a satisfactory chemical durability.

Some crystals were observed on the surface of MG45 after 2 weeks of immersion (Fig. 9A–C). The EDS spectrum (Fig. 9D) showed that these few large crystals, with an acicular shape (Fig. 9C), were rich in magnesium and phosphorous, while the matrix was rich of silicon,

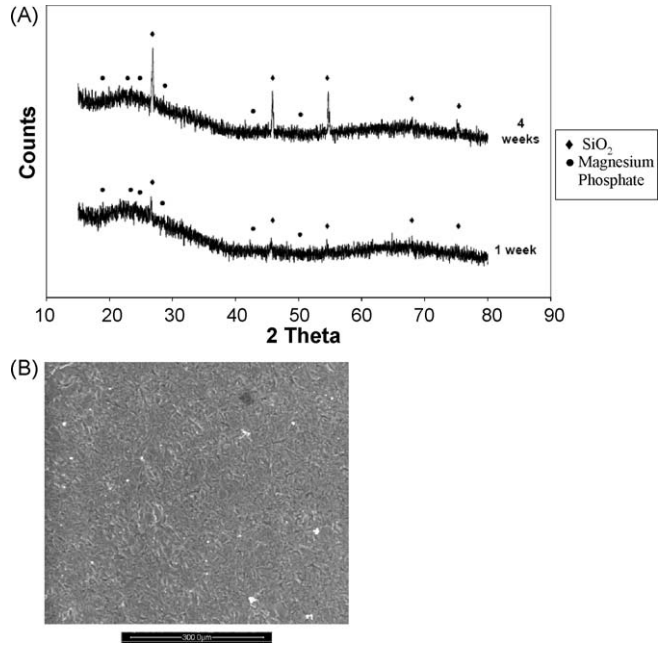

Fig. 13. (A) XRD spectra of MG45 after soaking in SBF. (B) SEM image of MG45 after 4 weeks of soaking in SBF.

magnesium, sodium and phosphorous. A little peak of calcium from the solution was also revealed (Fig. 9C). The XRD spectrum in Fig. 9E confirmed that the crystals were of magnesium phosphate (JCPDS 5-0579). Moreover, SiO_2 (JCPDS 79-1906) peaks were detected as the main phase. The MG45 glass surface possessed a silica-rich protective film, due to selective alkali ion removal (surface of type II), with very durable chemical characteristics, especially in solutions at pH lower than 9 [35]. Although Ca^{2+} ions were present in the incubation medium (HBSS+), calcium-containing salts were not detected on the surface of MG45. Therefore, it seems that in order to induce crystallisation of calcium phosphate on its surface, the glass has to contain calcium. It is worth noting that Kim et al. [4] were able to obtain bioactive glasses (immersed in SBF) even if P_2O_5 was absent in the glass composition. The present study suggests that calcium has to be included in the glass composition for apatite nucleation and growth (i.e. the bioactivity mechanism).

3.3.3. Microstructural analysis in HBSS−

After 4 weeks soaking in HBSS−, the solution free of calcium and magnesium ions, large crystals rich in calcium (Fig. 10A and B) and small rounded crystals rich in calcium and phosphorous (Fig. 10C and D) were present on the surface of BG45. The XRD graphs in Fig. 10E confirmed that the large crystals were of $CaCO_3$ (JCPDS 47-1743). The presence of a large amount of $CaCO_3$ crystals on the surface of BG45 after soaking in HBSS− could be due to the low solubility index of such crystals and to the composition of the solution (i.e. the presence of a large amount of HCO_3^-). The solubility index of $CaCO_3$ crystals was about 4.96×10^{-9} and the Hank's solution labelled HBSS− was rich of HCO_3^- ions (3.5 mM) (see Table 2). The small rounded crystals were of apatite, as confirmed by the EDS spectrum (Fig. 10D), with a Ca/P ratio of 1.86, close to the Ca/P ratio of 1.67 typical of crystalline hydroxyapatite. The matrix presented numerous cracks, due to the sodium release into the solution and to dissolution of the glass. Longer was the time of soaking, longer was the number and the size of crystals formed, for both $CaCO_3$ and apatite, even if the apatite crystals were always much smaller than those of $CaCO_3$. The XRD spectrum reported in Fig. 10E, after 1 and 4 weeks soaking, confirmed the presence of $CaCO_3$ (JCPDS 47-1743), apatite (JCPDS 73-1731) and SiO_2 (JCPDS 79-1906) crystals. The SiO_2 crystals were detected by XRD but not by ESEM since they were extremely small.

In conclusion, BG45 induced the formation of apatite crystals on its surface, even if the incubation solution was free of calcium ions.

Immediately after soaking in HBSS−, the surface of MG45 glass was corroded and some microcracks were visible in the matrix. After 1 and 2 weeks soaking the samples were quite vitreous, and no crystalline phase could be detected by X-rays (Fig. 11). After 4 weeks of soaking, ESEM revealed some large crystals, with the particular shape shown in Fig. 11A, similar to those of magnesium phosphate detected after soaking in HBSS+. The EDS microanalysis (Fig. 11B) and the XRD spectrum (Fig. 11C) confirmed that the crystals were magnesium phosphate (JCPDS 5-0579) and silica (JCPDS 79-1906). Thus, the crystalline phases detected by XRD on the surface of MG45 after 4 weeks of incubation in HBSS− were the same as that obtained in HBSS+. Apatite crystals were never observed. In conclusion, the MG45 glass, without calcium, after immersion in HBSS−, a solution without calcium, obviously did not have apatite crystals, but only magnesium phosphate and SiO_2 crystals on its surface.

3.3.4. Microstructural analysis in SBF

After 1 week immersion in SBF, numerous cracks and some crystals were visible on the surface of BG45 (Fig. 12A and B). The Ca/P ratio was of about 1.59 (EDS semi-quantitative analysis). After 4 weeks of soaking in SBF the surface was homogenously covered by rounded crystals (Fig. 12C), with a Ca/P ratio of 1.61, while the Ca/P ratio of the matrix was around 1.47 (Fig. 12D) (semi-quantitative EDS). The XRD spectrum (Fig. 12E) confirmed that the glass surface was covered by an apatite layer (JCPDS 73-1731) grown on a layer rich of SiO_2 (JCPDS 79-1906). Therefore, the BG45 surface had two layers of protective films, produced by precipitation of ions from the solution, and thus could be classified as a very durable surface of type III [35]. The microstructural behaviour of BG45 in SBF was similar to that observed in HBSS+, however the reactivity of BG45, in terms of apatite crystallisation, was higher in SBF. In conclusion, a solution with high concentration of calcium, such as SBF, would promote the apatite crystal formation.

The MG45, after soaking in SBF, presented a corroded surface due to a second stage reaction dissolution after

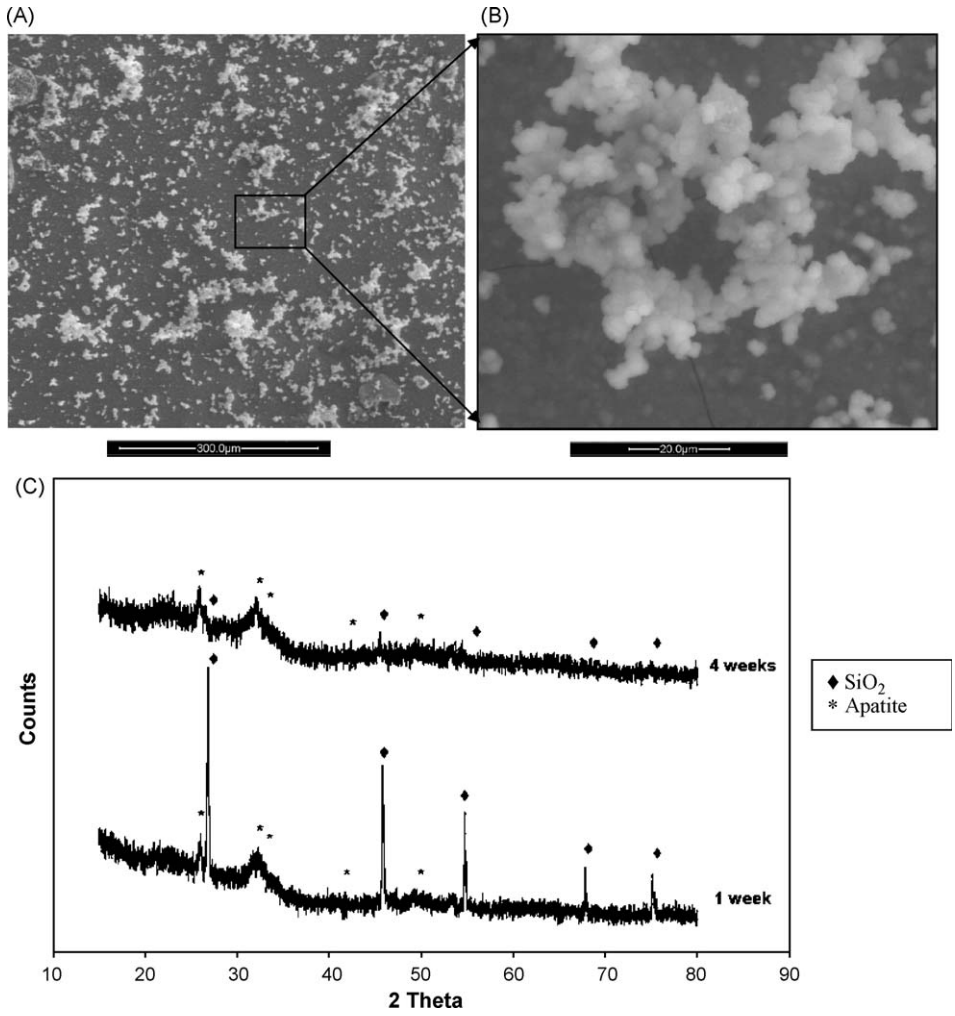

Fig. 14. (A and B) SEM images of BG45 flake surface after soaking in SBF after 4 weeks. (C) XRD spectrum of BG45 surface with flake shape after 1 week and 4 weeks of soaking in SBF. (D and E) SEM images of MG45 flake surface after soaking in SBF after 4 weeks. (F) XRD spectrum of MG45 surface with flake shape after 1 week and 4 weeks of soaking in SBF.

dealkalization of the surface and was vitreous up to the second week of soaking, as revealed by XRD (Fig. 13A). By contrast, crystals of SiO_2 (JCPDS 79-1906) and of magnesium phosphate (JCPDS 5-0579) were present on the glass surface after 4 weeks of soaking. ESEM was able to reveal only a few small crystals of magnesium phosphate, while SiO_2 crystals were smaller than the resolution power of the microscope (Fig. 13B). Apatite crystals were not detected by ESEM and X-rays. Therefore, the MG45 glass, not containing calcium ions, did not induced apatite crystallisation even if incubated in a calcium-rich solution. The microstructural behaviour of MG45 was similar in SBF and HBSS+. The MG45 surface, covered by a silica-rich protective film, was a surface of type II [35], very durable especially in solutions at pH < 9.

The effect of the roughness of the surface of the two glasses in SBF was investigated. The number of rounded particles formed on the surface of BG45 was much more elevated when the surface was of ''flake-type'' compared to flat (Fig. 14A and B). Both the crystals and the matrix were rich in calcium and phosphorous, suggesting that the whole surface was covered by a uniform apatite layer. The XRD spectrum confirmed that particles were hydroxyapatite crystals (JCPDS 73-1731) (Fig. 14C). SiO_2 (JCPDS 79-1906) crystals were present on the surface of BG45 only after the first 2 weeks of soaking. Later, SiO_2 crystals were not detected by XRD since the silica layer was completely covered by an apatite layer. Therefore, after soaking in SBF, the microstructural behaviour of BG45 in flake and flat form was qualitatively similar. The only differences were the quicker nucleation and the more numerous apatite crystals grown on flakes compared to flat surfaces. The effect of the morphology on the *in vitro* compatibility of bioactive glasses was previously reported in literature [23]. The present results seem to suggest that the superficial morphology affect the velocity of the apatite nucleation and crystallisation.

The MG45 glass surface in flake form showed a few cracks. After 4 weeks of immersion in SBF the MG45 in flake form presented some magnesium phosphate precipitates (Fig. 14D and E), while the matrix was phosphorous-free. Precipitates did not contain apatite, as confirmed by XRD (Fig. 14F) that detected only SiO_2 (JCPDS 79-1906) and magnesium phosphates (JCPDS 5-0579). The behaviour of MG45 in SBF in flat or flake form was qualitatively similar, since

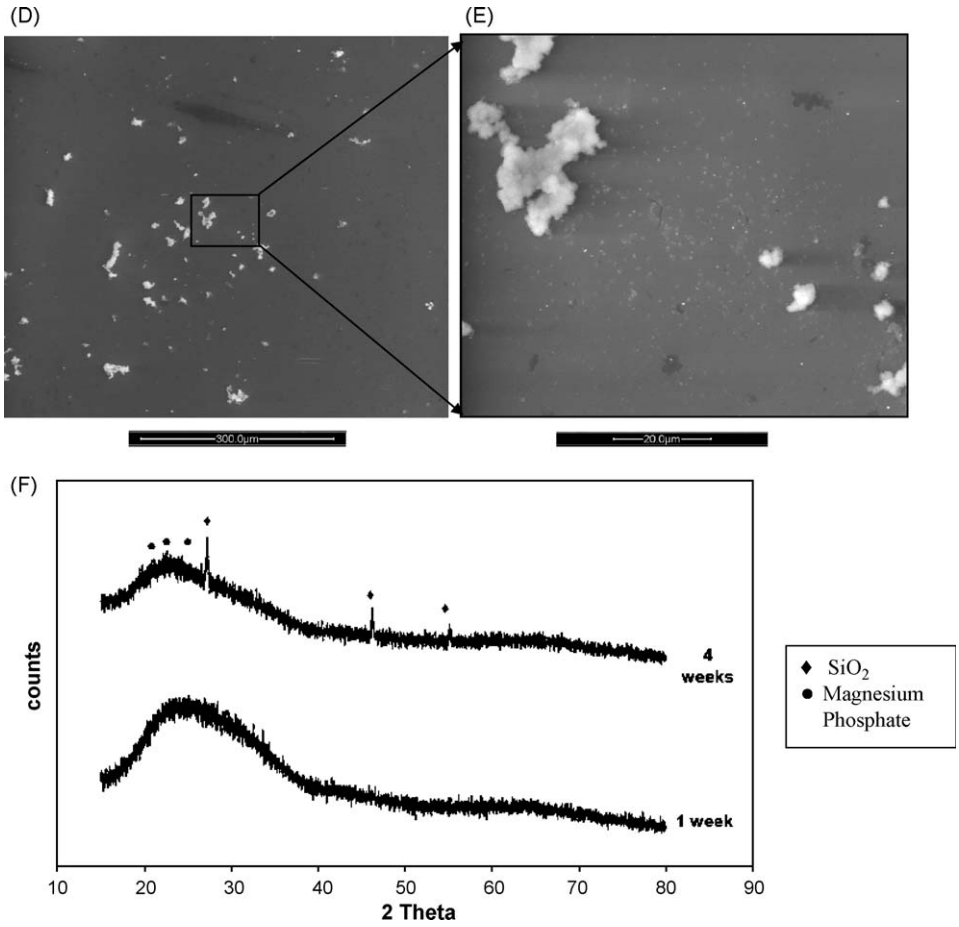

Fig. 14. (*Continued*).

crystalline phases were identical. However, the flake surface promoted crystallisation, as crystals grew faster and were larger.

4. Conclusions

In this study, two glasses, namely Hench's Bioglass® 45S5-labelled BG45 and a new glass based on the BG45 original composition with the complete substitution of CaO by MgO and labelled MG45, were analysed and compared.

The chemical durability and the *in vitro* behaviour of such glasses after soaking up to 4 weeks at physiological temperature in bi-distilled water and in different simulated biological fluids were evaluated. In particular, glasses were incubated in Hanks' Buffered Salt Solution 61200 (HBSS+), containing calcium and magnesium, in Hanks' Buffered Salt Solution 14170 (HBSS−), free of calcium and magnesium, and in Kokubo's Simulated Body Fluid (SBF). Glasses were carefully characterised before and after different treatments in order to determine their dissolution and the reactions occurring at their surfaces. The influence of the surface morphology of both glasses incubated in SBF was also investigated.

MG45 seemed to be more thermally stable in comparison with BG45, since no crystallisation temperature was detected in MG45 by DTA. Moreover, the chemical durability of MG45 glass was higher than that of BG45 in water and SBF.

However, the findings of the present study indicate that the chemical durability of a glass immersed into a water saline at 37 °C depends mainly on the chemical composition of the soaking solution.

The HBSS− solution was less efficient than HBSS+ in inducing the formation of apatite on BG45. The Ca/P ratio of 1.86, obtained after 4 weeks of soaking in HBSS−, was close to that of about 1.80 obtained after only 1 week of soaking in HBSS+. Indeed, SBF was the most reactive solution. In fact, SBF induced the formation of apatite crystals on the surface of BG45 in a shorter time compared to other solutions.

On the contrary, HBSS+ and SBF, although rich in calcium ions, were unable to induce the formation of apatite crystals on the surface of MG45, even after 4 weeks soaking, and independently from the roughness of the samples surface.

Different solutions induced different crystalline phases in different proportions on the surface of both glasses. For BG45, the main crystalline phase present after immersion in all the solutions was SiO_2 (JCPDS 79-1906), according to the well-known mechanism of bioactive glasses which involves the formation of a silica layer on the surface of the glass on which apatite can grow [2]. As secondary phases, apatite

(JCPDS 73-1731) and calcium carbonate (JCPDS 47-1743) were detected on the surface of BG45. The apatite crystallisation could be attributed to the reactions of the glass with different solutions, while $CaCO_3$ crystallisation was attributed to atmospheric CO_2, after soaking in bi-distilled water, and to the composition of the solution, containing HCO_3^- after immersion in HBSS−. BG45 was therefore a bioactive material, as known from literature, since the apatite layer could be seen after soaking in different simulated biological fluids [2].

An apatite layer was never seen on the surface of MG45 glass even if incubated for 4 weeks in solutions containing calcium and magnesium. The crystalline phases detected on the MG45 surface after immersion in different solutions were only SiO_2 (JCPDS 79-1906) and magnesium phosphate (JCPDS 5-0579). Therefore, in order to induce the formation of apatite on the surface of a glass as a reactivity of the glass-solution system, the glass itself should contain calcium.

As regards the effect of the solution used, the bi-distilled water was the less reactive medium for the BG45 glass. Moreover, the chemical durability of BG45 was higher in HBSS− than in HBSS+, since the apatite crystallisation was more active in HBSS+. The reactivity of BG45 was higher in SBF than in the other solutions, and SBF favoured the apatite crystallisation. Therefore, the presence of high quantity of calcium in the soaking solution, such as SBF, promotes the formation of apatite crystals on glasses already containing calcium.

The bioactive mechanism in SBF of BG45 was similar on both flat and flake samples, even if the amount and the size of crystals increased on flake samples. Therefore, the present results confirm that the morphology of the surface of glasses influenced nucleation and growth of crystals as the roughness being a promoter of crystallisation.

Acknowledgements

The authors would like to thank Dr. M.A. Croce (University of Modena and Reggio Emilia, Italy) for the help in performing the *in vitro* tests. A. Gupta (Indian Institute of Technology, Kanpur, India) is acknowledged for his collaboration. Thanks also to Dr. M. Cannio for help with the ICP-AES testing.

References

[1] L.L. Hench, Bioceramics: from concept to clinic, Journal of American Ceramic Society 74 (1991) 1487–1510.
[2] L.L. Hench, Bioceramics, Journal of American Ceramic Society 81 (1998) 1705–1728.
[3] Clerk, L.L. Hench, The influence of surface chemistry on implant interface, Journal of Biomedical Materials Researches 10 (1976) 161–174.
[4] H.M. Kim, F. Miyaji, T. Kokubo, Bioactivity of Na_2O–CaO–SiO_2 glasses, Journal of American Ceramic Society 78 (1995) 2405–2411.
[5] E.E. Stroganova, N.Yu. Mikhailenko, O.A. Moroz, Glass-based biomaterials: present and future (a review), Glass and Ceramics 60 (2003) 315-.
[6] E. Jallot, Role of magnesium during spontaneous formation of a calcium phosphate layer at the periphery of a bioactive glass coating doped with MgO, Applied Surface Science 211 (2003) 89–95.
[7] F. Barrere, C.A. van Blitterswijk, K. De Groot, P. Layrolle, Influence of ionic strength and carbonate on the Ca–P coating formation from SBF X 5 solution, Biomaterials 23 (2002) 1921.
[8] H.L. Ren, Y. Yue, C.H. Ye, L.P. Guo, J.H. Lei, NMR study of crystallisation in MgO–CaO–SiO_2–P_2O_5 glass–ceramics, Chemical Physics Letters 2982 (1998) 317–322.
[9] S. Agathopoulos, D.U. Tulyaganov, J.M.G. Ventura, S. Kannan, M.A. Karakassides, J.M.F. Ferreira, Formation of hydroxyapatite onto glasses of the CaO–MgO–SiO_2 system with B_2O_3, Na_2O, CaF_2 and P_2O_5 additives, Biomaterials 27 (2006) 1832–1840.
[10] W. Holand, Biocompatible and bioactive glass–ceramics—state of the art and new directions, Journal of Non-Crystalline Solids 219 (1997) 192–197.
[11] V.K. Marghussian, A. Sheikh-Mehdi Mesgar, Effects of composition on crystallization behaviour and mechanical properties of bioactive glass–ceramics in the MgO–CaO–SiO_2–P_2O_5 system, Ceramics International 26 (2000) 415–420.
[12] V. Banchet, J. Michel, E. Jallot, L. Worthman, S. Bouthors, D. Laurent-Maquin, G. Balossier, Interfacial reactions of glasses for biomedical application by scanning transmission electron microscopy and microanalysis, Acta Biomaterialia 2 (2006) 349–359.
[13] J.M. Oliveira, R.N. Correia, M.H. Fernandes, Surface modifications of a glass and a glass–ceramic of the MgO–3CaO*P_2O_5–SiO_2-system in a simulated body fluid, Biomaterials 16 (1995) 849–854.
[14] R.Z. Legeros, R. Kijkowska, I. Kattech, M. Jemal, J.P. Legeros, Journal of Dental Research 65 (1986) 783.
[15] I. Barrios de Arenas, C. Schattner, M. Vasquez, Bioactivity and mechanical properties of $Na_2O.CaO.SiO_2.P_2O_5$ modified glass, Ceramics International 32 (2006) 515–520.
[16] W. Cao, L.L. Hench, Bioactive materials, Ceramics International 22 (1996) 493–507.
[17] P.N. De Aza, A.H. De Aza, P. Pena, S. De Aza, Bioactive glass and glass–ceramics, Ceramica y Vidro Bolletin Sociedad Espanola Ceramica 46 (2) (2007) 45–55.
[18] M. Cerruti, D. Greenspan, K. Powers, Effect of pH and ionic strength on the reactivity of Bioglass 45S5, Biomaterials 26 (2005) 1665–1674.
[19] M. Cerruti, C.L. Bianchi, F. Bonino, A. Damin, A. Perardi, C. Morterra, Surface modifications of bioglass immersed in TRIS buffered solutions. A multitechnical spectroscopy study, The Journal of Physical Chemistry B 109 (2005) 14496–14505.
[20] A.K. Varshneya, Fundamentals of Inorganic Glasses, Academic Press, Boston, 1993.
[21] T. Kokubo, H. Takadama, How useful is SBF in predicting in vivo bone bioactivity? Biomaterials 27 (2006) 2907–2915.
[22] J.H. Hanks, R.E. Wallace, Proceedings of the Society for Experimental Biology and Medicine 71 (1949) 196.
[23] A.L. Andrade, P. Valerio, A.M. Goes, M.F. Leite, R.Z. Domingues, Influence of morphology on in vitro compatibility of bioactive glasses, Journal of Non-Crystalline Solids 2352 (2006) 3508–3511.
[24] M.B. Volf, Chemical Approach to Glass, Elsevier, 1984.
[25] K. Shimoda, T. Nemoto, K. Saito, Local structure of magnesium in silicate glasses: a ^{25}Mg 3QMAS NMR study, Journal of Physical Chemistry B 112 (2008) 6747–6752.
[26] A.Z. Dietzel, Die Kationenfeldstirken und ihre Beziehungen zu Entglasungsvorgangen, zur Verbindungsbildung und zu den Schmelzpunkten von Silikaten, Z Elektrochemie 48 (1942) 9–23.
[27] K.-H. Sun, Fundamental condition of glass formation, Journal of the American Ceramic Society 30 (1947) 277.
[28] H.A. ElBatal, M.A. Azooz, E.M.A. Khalil, A.S. Monem, Y.M. Hamdy, Characterisation of some bioglass–ceramics, Materials Chemistry and Physics 80 (2003) 599–609.
[29] L. Lefebre, J. Chevalier, L. Gremillard, R. Zenati, G. Thollet, D. Bernache-Assolant, A. Govin, Structural transformations of bioactive glass 45S5 with thermal treatments, Acta Materialia 55 (2007) 3305–3313.
[30] A.R. Boccaccini, Q. Chen, L. Lefebre, L. Gremillard, J. Chevalier, Sintering, crystallisation and biodegradation behaviour of Bioglass®-derived glass–ceramic, Faraday Discussions 136 (2007) 27–44.

[31] T.R. Zeitler, A.N. Cormack, Interaction of water with bioactive glass surfaces, Journal of Crystal Growth 294 (2006) 96–102.
[32] R.K. Iler, The Chemistry of Silica, Wiley, New York, 1979.
[33] D.S. Brauer, C. Russel, J. Kraft, Solubility of glasses in the system P_2O_5–CaO–MgO–Na_2O–TiO_2: experimental and modeling using artificial neural networks, Journal of Non-Crystalline Solids 353 (2003) 263–270.
[34] A.B. Jedlicka, A.G. Clare, Chemical durability of commercial silicate glasses. I. Material characterisation, Journal of Non-Crystalline Solids 281 (2001) 6–24.
[35] L.L. Hench, D.E. Clark, Physical chemistry of glass surfaces, Journal of Non-Crystalline Solids 28 (1978) 83.
[36] D.E. Clark, E.L. Yen-Bower, Corrosion of glass surfaces, Surface Science 100 (1980) 53–70.